GEOPHYSICS, VOL. 80, NO. 3 (MAY-JUNE 2015); P. A69–A73, 3 FIGS.
10.1190/GEO2014-0437.1

Variable source depth acquisition for improved marine broadband seismic data

Kjetil E. Haavik[1] and Martin Landrø[1]

ABSTRACT

In marine seismic data acquisition, varying the source depth along a sail line gives diversity in sequential shot gather frequency spectra. Undesired alterations of the frequency spectra are created by the source ghost and by air-gun bubble oscillations. By deliberately varying the source depth along a sail line, it is possible to obtain a seismic data set that will have energy more evenly distributed within the main frequency band of the source output. This is obtained when data acquired with different source depths are stacked in imaging. We formulated a simple inverse problem that seeks to find the optimal distribution of source depths over a sequential series of shots that shape the amplitude spectrum of the final image into a desired shape. We assumed that the data are receiver-side deghosted, that designature could be applied to each shot gather, and that the shot gathers could be redatumed to a common datum prior to imaging.

INTRODUCTION

Recent interest in broadband seismic, and especially the low-frequencies end, has triggered several seismic acquisition solutions. Increasing the bandwidth of the seismic signal in the low end of the frequency spectrum improves penetration and resolution in reflection seismic data, and it is beneficial in waveform and impedance inversion (ten Kroode et al., 2013). Marine seismic acquisition systems that provide seismic data with broader bandwidth have been developed, and the most important feature of these systems is their ability to eliminate the ghost reflections from the free surface. The ghost reflections cause deep notches in the amplitude spectra of the recorded data at frequencies determined by the depths of the source and the receivers. Improvements in positioning systems, recording devices, computer power, and new processing algorithms are probably the most important factors that have made it possible to realize older ideas for dealing with the ghost (e.g., Berni, 1982; Ray and Moore, 1982; Sonneland and Berg, 1985). For the receiver side, broadband acquisition systems can be divided into two main categories: (1) multicomponent recordings (e.g., Loewenthal et al., 1985; Robertsson et al., 2008; Vaage et al., 2008; Day et al., 2013) and (2) slanted streamer profiles (e.g., Ray and Moore, 1982; Soubaras and Dowle, 2010; Seymour et al., 2012), which allows for deghosting by wavefield separation and deconvolution, respectively. However, deghosting of conventional seismic data, i.e., pressure measurements at constant streamer depth, also result in improvements of the final image compared with nondeghosted data (Zhou et al., 2012; Dhelie et al., 2014). The source-side deghosting algorithms used today rely on predictive deconvolution and/or using multilevel sources to avoid the notches introduced by the ghost reflection (Moldoveanu, 2000; Hopperstad et al., 2008; Halliday, 2013; Sablon et al., 2013).

Here, we present a new strategy for acquiring seismic data for improving the ghost notch and bubble notch diversity related to the air-gun source. As a reciprocal experiment to the slanted streamer, the source depth is varied along a sail line to obtain notch diversity in the amplitude spectra. Furthermore, by choosing the source depths carefully, it is possible to optimize the shape of the frequency spectrum for the final seismic image.

THEORY

Notches in the air-gun spectrum

The acoustic signal generated by an air gun has been studied extensively (Giles, 1968; Ziolkowski, 1970; Ziolkowski et al., 1982; Vaage et al., 1983; Landrø et al., 2011; Barker and Landrø, 2013).

Manuscript received by the Editor 17 September 2014; revised manuscript received 22 November 2014; published online 27 March 2015.
[1]Department of Petroleum Engineering and Applied Geophysics, Trondheim, Norway. E-mail: kjetil.haavik@ntnu.no; martin.landro@ntnu.no.

The low-frequency output from an air-gun array is primarily related to the bubble that expands and contracts several times before it dissolves or breaks the air-water interface. The bubble time period is dependent on the firing pressure P, air-gun volume V, and source depth z in meters, and it is given by the Rayleigh-Willis formula (Rayleigh, 1917; Willis, 1941):

$$\tau = \text{const.}\,\frac{P^{\frac{1}{3}}V^{\frac{1}{3}}}{(10+z)^{\frac{5}{6}}}. \tag{1}$$

The low-frequency output will have a maximum at the frequency $f_b = \tau^{-1}$. The bubble also creates notches, or depressions, in the frequency spectrum that are periodically related to the bubble time period as (Landrø and Amundsen, 2014)

$$f_{bn} = \frac{n+\frac{1}{2}}{\tau}, \qquad n = 0, 1, 2, \ldots. \tag{2}$$

Interference between the primary downgoing wavefield and wavefield reflected at the free surface causes notches in the frequency spectrum. Assuming that the signal is recorded vertically below the air gun, the notches are positioned at the frequencies given by

$$f_{gn} = \frac{c}{2z}n, \quad n = 0, 1, 2, \ldots, \tag{3}$$

where c is the sound velocity of water and z is the source depth in meters. The far-field amplitude spectrum from an air gun will have notches related to bubble oscillations and the free surface. The notches or depressions in the frequency spectra caused by bubble oscillations are small compared with the severe notches caused by the ghost reflection. This is because a tuned air-gun array has a diversity of bubble periods. The severity of these notches and depressions depends on the free-surface reflection coefficient for the ghost notches and the primary to bubble ratio for the bubble related notches, respectively. The low-frequency output from an air-gun array is almost unaffected by the source depth (Hegna and Parkes, 2011; Hopperstad et al., 2012; Landrø and Amundsen, 2014). There are two major effects related to the depth of the source that influences the low-frequency output from an air gun. The bubble time period increases as the source depth decreases resulting in more low-frequency energy. However, the change in ghost response due to the same decrease in source depth will counteract that increase in low-frequency output. Hopperstad et al. (2012) show even greater constraints on the low-frequency output from an air-gun cluster: The output well below the lowest bubble resonance frequency is only determined by the total quantity of air released, i.e., the product of firing pressure and the total volume.

Inverting for optimal source depths

Acquiring seismic data with a constant source depth will result in a data set that contains notches due to the ghost reflection and the bubble oscillations at the same frequencies throughout the data set. To avoid this, we suggest to use various source depths along sail lines. Our objective is to obtain a data set that, over a sequence of shots, has energy distributed equally among all frequencies in the final image. If we, for simplicity, only consider the signal propagating vertically from the source, the total frequency spectrum of the final stacked image from combining data acquired with N different and predefined source depths is given as

$$\mathbf{s}(f) = \sum_{i=1}^{N} a_i \mathbf{k}_i(f), \tag{4}$$

where k_i is the vertical far-field amplitude spectrum from the source fired at depth i, f is the frequency, and a_i is a weight factor for the ith source depth. The choice of a_i will determine the shape of the total frequency spectrum and a_i is used to find the number of sources that should be positioned at depth z_i in a shot sequence. Equation 4 can be written in matrix notation as $\mathbf{s} = \mathbf{Ka}$.

We formulate an inverse problem that seeks to find the set of a_i that shape the frequency spectrum $\mathbf{s}$ of the final image into a desired frequency spectrum $\mathbf{s_d}$. We define the objective function for this inverse problem as

$$\Phi(\mathbf{a}) = \Phi_d(\mathbf{a}) + \beta\Phi_m(\mathbf{a}), \tag{5}$$

where $\mathbf{a}$ is the model vector that contains the weights, Φ_d is the data objective function, β is a regularization parameter (Tikhonov and Arsenin, 1977), and Φ_m is the model objective function. We use the standard least-squares norm for the data and model objective functions, respectively,

$$\Phi_d(\mathbf{a}) = \frac{1}{2}\|\mathbf{W}_d(\mathbf{Ka} - \mathbf{s}_d)\|^2, \tag{6}$$

$$\Phi_m(\mathbf{a}) = \frac{1}{2}\|\mathbf{W}_m\mathbf{a}\|^2, \tag{7}$$

where $\mathbf{W}_d$ is the data weighting matrix and $\mathbf{K}$ is a matrix containing the kernel functions. The kernel functions for this problem are the amplitude spectra for vertical far-field source signatures from the source fired at different depths. The $\mathbf{W}_m$ is a weighting matrix in model space. Here, we use $\mathbf{W}_m$ as the differential operator that will penalize rapid variation in $\mathbf{a}$. This is done for practical reasons because we would like to have a smooth transition between the different source depths during acquisition. A solution that minimizes the objective function in equation 5 with respect to $\mathbf{a}$ is the classical least-squares solution given in, e.g., Oldenburg and Li (2005) as

$$\mathbf{a} = (\mathbf{K}^T\mathbf{W}_d^T\mathbf{W}_d\mathbf{K} + \beta\mathbf{W}_m^T\mathbf{W}_m)^{-1}(\mathbf{K}^T\mathbf{W}_d^T\mathbf{W}_d\mathbf{s}_d). \tag{8}$$

We suggest to design a sequence of source depths (SSD) that will result in an amplitude spectrum of a desired shape. The number of shots within the SSD times an integer should be equal to the common midpoint (CMP)-fold to ensure that all CMPs contain data from all source depths within an SSD. It is clear that the depths of sequential sources must be close to make the necessary changes in source depth as smooth and simple as possible. There might be several potential practical solutions to achieve this, but what we foresee is a source depth controller that continuously moves sources up and down in a gentle and smooth manner.

OPTIMAL SOURCE DEPTHS USING FIELD DATA

A field experiment was conducted in a Norwegian fjord a few years ago (Landrø and Amundsen, 2014). A single 600 in^3 air gun was used as source. The water depth at the location is approximately 390 m, and the weather conditions were excellent during tests. The source was positioned at approximately 3, 5, 7, 10, 15, 20, 25, 30, 35, and 40 m, and a hydrophone was positioned 20 m below the source. The far-field signatures for sources fired at different depths were estimated by the notional source method (Ziolkowski et al., 1982) and then convolved with the source ghost functions for the respective source depths. The data were filtered with a high-cut filter (230–250 Hz) and normalized to the highest amplitude. The estimated far-field signatures are shown in Figure 1. The far-field signatures in Figure 1 show the expected characteristics from sources fired at different depths. The primary pulse is aligned for all source depths (white spike at approximately 0.025 s), and the ghost reflection is seen as the black spike following the primary pulse and is deviating more as the source depths are increasing. The first bubble can be seen at approximately 0.2 s for the first trace, and it is shifted toward earlier times as the source depths increase.

We perform two inversions as described in equation 8, one with regularization ($\beta \neq 0$) and the second without regularization. The kernel matrix $\mathbf{K}$ contains the frequency spectra of the estimated vertical far-field signatures from each depth, and the identity matrix was used for the data weighting matrix $\mathbf{W}_d$. For the desired spectrum $\mathbf{s}_d$, we use a white spectrum within the frequency band of interest (0–250 Hz). We would like to find the combinations of source depths that will give the flattest amplitude spectrum using 40 shots. The results from these inversions are compared with the amplitude spectrum of a multilevel source that consists of two air guns at 6 and 9 m and have strengths equivalent to two-thirds and one-third of the air gun used in the inversion, respectively. Because there are no records from sources fired at 6 and 9 m, we use the notional source signature from the sources fired at 5 and 10 m and then convolved them with the ghost response for 6 and 9 m, respectively, and tuned them on peak. This will not give the correct bubble time period, but it will give the amplitude spectra closest to the much-used 6 and 9 m configuration. The inversion results are shown in Figure 2, and the corresponding distribution of source depths is shown in Figure 3.

The inversion results in Figure 2 show that the variable source depths (blue and black curves) give whiter amplitude spectra than the multilevel source (red curve). The ghost notches corresponding to source depths of 6 and 9 m are 125 and 83 Hz, respectively, and we observe a large difference in amplitudes between the multilevel source and the inversion results in the vicinity of those frequencies. We observe a significant improvement also for low frequencies, especially at approximately 10 Hz, where the inversion results show an improved amplitude response of up to 12 dB. The notch at approximately 10 Hz, and oscillating behavior observed in the

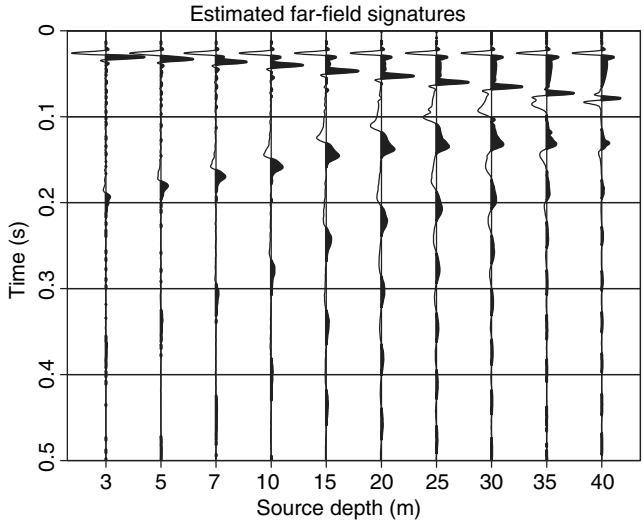

Figure 1. The estimated far-field signatures for zero offset from a single 600 in^3 air gun fired at depths ranging from 3 to 40 m. Note how the bubble pulse delay is reduced as the source depth increases. Also note the free-surface ghost and how it is delayed as the source depth increases.

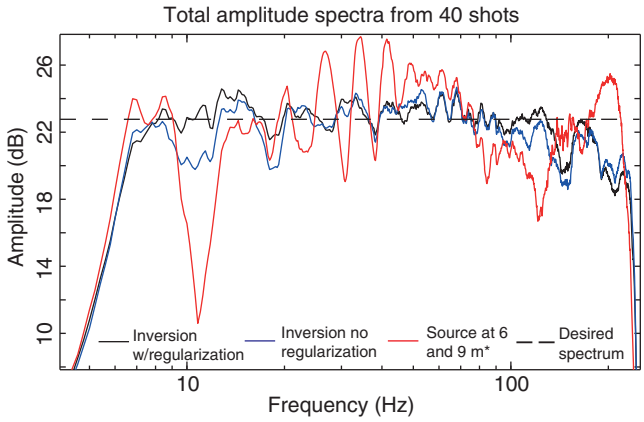

Figure 2. The total amplitude spectra from combining data from air guns fired at different depths. The black and blue curves are the amplitude spectra from the inversion with and without regularization, respectively. The red curve is the amplitude spectrum from a multilevel source with sources at 6 and 9 m. Because no source signatures were recorded from sources at 6 and 9 m, we estimate these far-field signatures by convolving the notional source signatures from 5 and 10 m with the ghost response for source depths of 6 and 9 m, respectively, hence, the star.

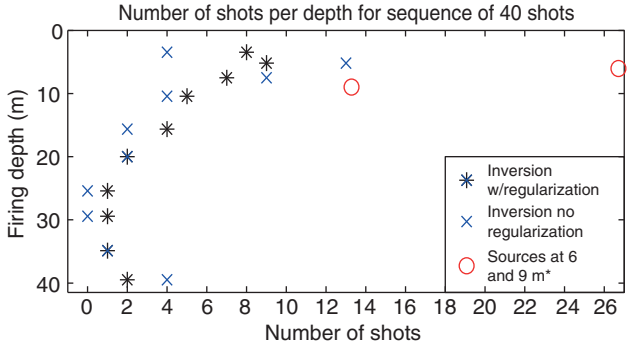

Figure 3. The number of shots per source depth in a sequence of 40 shots. The red circles represent the equivalent distribution of strength in a multilevel source with air guns at depths of 6 and 9 m.

spectrum of the multilevel source is a result of the bubble oscillations. This behavior is far less pronounced in the amplitude spectra estimated from the inversion. The cause for this is the diversity of bubble notches as multiple source depths are included. The amplitudes from the multilevel source from 3 to 9 Hz are approximately 0.5 dB higher, with a maximum difference of approximately 2.5 dB at 7.5 Hz, compared with the amplitudes from the constrained inversion result (black curve). In the frequency band between 170 and 230 Hz, we find that the amplitude response from the multilevel source is better than the inversion result. The optimal source depths (Figure 3) obtained by inversion show that approximately 50% of the shots should be fired at depths in the range of 3.4–7.5 m, and only 15% should be deeper than 15 m. This result aligns well with the discussion in Landrø and Amundsen (2014).

DISCUSSION

We use the amplitude spectrum resulting from combining data acquired for different source depths for the same take-off angle (vertical). However, a CMP gather contains a signal that left the source with other take-off angles. The optimal source depths in a SSD should therefore be modeled for a specified target. In general, the effect of directivity will influence shallow targets more than deep targets if this is not taken into account in survey design.

To be able to benefit the most from variable source depth acquisition (VSDA), each shot gather needs to be redatumed to a common datum, and designature and deghosting should be applied. The two latter processes involve spectral shaping of the data and are fairly common processing steps in modern seismic processing. The term *designature* often includes debubbling and deghosting. The debubble process is stable because the bubble notches or depressions are small compared with the severe ghost notches. However, the result of debubbling is dependent on a good estimate of the source signature. The source-side deghosting process consists of deconvolving the recorded data with the ghost response. This process is unstable in the vicinity of the ghost notches, where we have a poor signal-to-noise ratio (S/N) and where we, in practice, divide by zero. If the same source depth is used throughout a seismic survey, it will lead to a data set that suffers from a poor S/N in the vicinity of these frequencies, and we are in a way repeating the same error every shot. VSDA as proposed here will ensure that the final data set has energy distributed more evenly among the frequency band of the source output. Except for the notch present at 0 Hz common for all source depths, notch diversity will ensure that there are no frequency bands within our main signal that have poorer signal to noise ratio than others; i.e., we are not repeating the error. The deghosting process is theoretically sound, but it suffers from a division by zero at the ghost notch frequencies. VSDA is a way to optimize seismic data for processing during acquisition, rather than to do it all during processing.

Seismic data acquired with variable source depths will not give a substantial difference on the low-frequency end (less than 6 Hz) of the frequency spectrum compared with other air-gun source configurations. The low-frequency response from an air-gun array is only weakly dependent on the source depth. If we position the source deeper, it will result in a source ghost response more favorable for the low frequencies, but the corresponding reduction in the bubble time period yields less low-frequency output (Hegna and Parkes, 2011; Hopperstad et al., 2012; Landrø and Amundsen, 2014). However, the main effect and goal of this acquisition strategy is to obtain diversity of the notches related to the ghost and notches or depressions caused by the bubble. The field data studied here are from a single 600 in^3 air gun, and the bubble is therefore more pronounced compared with a tuned air-gun array. Still, it is possible to obtain a fairly white spectra. We think that the combination of VSDA and large sources, such as the hypercluster (Hopperstad et al., 2012) will yield data sets that have more low-frequency energy and that this can be exploited to improve marine broadband seismic data.

The inversion presented here requires knowledge of the source signatures from each of the source depths. These source signatures should have a high S/N, and ideally be noise free, to prevent the influence of noise in the inversion. Available for this study, we have recordings from a single large air gun fired at depths ranging from 3 to 40 m. This method is not restricted to using a single air gun; as long as the source signatures are known, this method can be used. An alternative to measuring the signatures may be to model them for the different depths. More sophisticated inversions can include source signature modeling as a forward model in an iterative scheme. In such a scheme, more model parameters, such as number of air guns, pressure, and total volume can be included. However, we choose to use the simple inversion here to illustrate the main point of VSDA.

CONCLUSIONS

We suggest gradually changing the source depth along sail lines during acquisition to introduce diversity of the notches and depressions in the frequency spectra caused by the ghost reflection and the bubble oscillation, respectively. Using an inversion to find the optimal source depths over a sequential series of shots, we obtain an amplitude spectrum in the final image that is close to a desired and predefined shape. Here, we specify a white spectrum within the frequency band of the source output as the desired spectrum. The desired shape can be changed to accommodate other shapes, but the final shape is always limited by the bandwidth of the source used.

Based on the recorded seismic data obtained from firing a large single air gun at various source depths, we show that it is possible to use an inversion technique to obtain an optimal sequence of shot depths to produce a close-to-white frequency spectrum. When comparing the spectrum from a 6- to 9-m multilevel source with the total spectrum of an optimal SSD over 40 shots, we find that the variable source depth spectrum has energy that is more evenly distributed.

ACKNOWLEDGMENTS

Thanks go to Lundin Norway AS for the financial support of K. E. Haavik's Ph.D. project. We acknowledge Statoil ASA for contributing with the seismic source recordings. Å. S. Pedersen and M. Thomson are acknowledged for designing and conducting the field work. P. E. Dhelie at Lundin Norway AS is acknowledged for useful comments and suggestions that improved this paper. The associate editor J. Rickett and two reviewers, including J. F. Hopperstad and one anonymous, are acknowledged for valuable and constructive feedback that have improved this manuscript. M. Landrø thanks the Norwegian Research Council for financial support.

REFERENCES

Barker, D., and M. Landrø, 2013, Estimation of bubble time period for air-gun clusters using potential isosurfaces: Geophysics, **78**, no. 4, P1–P7, doi: 10.1190/geo2012-0344.1.

Berni, A. J., 1982, Marine seismic system: U.S. Patent, 4,520,467.
Day, A., T. Klüver, W. Söllner, H. Tabti, and D. Carlson, 2013, Wavefield-separation methods for dual-sensor towed-streamer data: Geophysics, **78**, no. 2, WA55–WA70, doi: 10.1190/geo2012-0302.1.
Dhelie, P. E., J. Lie, V. Danielsen, and A. Myklebostad, 2014, Broadband for everyone — Increasing notch diversity using variable streamer profiles: 76th Annual International Conference and Exhibition, EAGE, Extended Abstracts, TuELI213.
Giles, B. F., 1968, Pneumatic acoustic energy source: Geophysical Prospecting, **16**, 21–53, doi: 10.1111/j.1365-2478.1968.tb01959.x.
Halliday, D. F., 2013, Source-side deghosting: A comparison of approaches: 83rd Annual International Meeting, SEG, Expanded Abstracts, 67–71.
Hegna, S., and G. Parkes, 2011, The low frequency output of marine air-gun arrays: 81st Annual International Meeting, SEG, Expanded Abstracts, 77–81.
Hopperstad, J. F., R. Laws, and E. Kragh, 2008, Fundamental principles of isotropic marine source design: 70th Annual International Conference and Exhibition, EAGE, Extended Abstracts, B025.
Hopperstad, J. F., R. Laws, and E. Kragh, 2012, Hypercluster of airguns more low frequencies for the same quantity of air: 74th Annual International Conference and Exhibition incorporating SPE EUROPEC, EAGE, Extended Abstracts, Z011.
Landrø, M., and L. Amundsen, 2014, Is it optimal to tow air guns shallow to enhance low frequencies?: Geophysics, **79**, no. 3, A13–A18, doi: 10.1190/geo2013-0348.1.
Landrø, M., L. Amundsen, and D. Barker, 2011, High-frequency signals from air-gun arrays: Geophysics, **76**, no. 4, Q19–Q27, doi: 10.1190/1.3590215.
Loewenthal, D., S. S. Lee, and G. H. F. Gardner, 1985, Deterministic estimation of a wavelet using impedance type technique: Geophysical Prospecting, **33**, 956–969, doi: 10.1111/j.1365-2478.1985.tb00791.x.
Moldoveanu, N., 2000, Vertical source array in marine seismic exploration: 70th Annual International Meeting, SEG, Expanded Abstracts, 53–56.
Oldenburg, D. W., and Y. Li, 2005, Inversion for applied geophysics: A tutorial, *in* D. Butler, ed., Near-surface geophysics, SEG, Investigations in Geophysics Series, no. 13, 89–150.
Ray, H. C., and N. A. Moore, 1982, High resolution, marine seismic stratigraphic system: U.S. Patent, 4,353,121 A.
Rayleigh, L., 1917, On the pressure developed in a liquid during the collapse of a spherical cavity: Philosophical Magazine, **34**, 94–98, doi: 10.1080/14786440808635681.
Robertsson, J. O. A., I. Moore, M. Vassallo, K. Özdemir, D. van Manen, and A. Özbek, 2008, On the use of multicomponent streamer recordings for reconstruction of pressure wavefields in the crossline direction: Geophysics, **73**, no. 5, A45–A49, doi: 10.1190/1.2953338.
Sablon, R., T. Payen, H. Tonchia, R. Siliqi, X. Labarre, N. Salaun, and Y. L. Men, 2013, Ghost-free imaging combining synchronized multi-level source and variable-depth streamer: 83rd Annual International Meeting, SEG, Expanded Abstracts, 72–76.
Seymour, N. M. N., D. Manen, and P. Caprioli, 2012, Broadband seismic methods for towed streamer acquisition: 74th Annual International Conference and Exhibition incorporating SPE EUROPEC, EAGE, Extended Abstracts, Z009.
Sonneland, L., and L. E. Berg, 1985, A new method for separating wavefields in to up-and down-going components: Presented at 47th EAEG Meeting.
Soubaras, R., and R. Dowle, 2010, Variable-depth streamer — A broadband marine solution: First Break, **28**, 1328–1335.
ten Kroode, F., S. Bergler, C. Corsten, J. W. de Maag, F. Strijbos, and H. Tijhof, 2013, Broadband seismic data the importance of low frequencies: Geophysics, **78**, no. 2, WA3–WA14, doi: 10.1190/geo2012-0294.1.
Tikhonov, A. V., and V. Y. Arsenin, 1977, Solution of ill-posed problems: John Wiley and Sons, Inc.
Vaage, S., K. Haugland, and T. Utheim, 1983, Signatures from single air-guns: Geophysical Prospecting, **31**, 87–97, doi: 10.1111/j.1365-2478.1983.tb01043.x.
Vaage, S. T., S. T. Tengham, and C. N. Borresen, 2008, System for combining signals of pressure signals and particle motion sensors in marine seismic streamers: U.S. Patent, 7,359,283 B2.
Willis, H., 1941, Underwater explosions, time interval between successive explosions: British report WA-47-21.
Zhou, Z., M. Cvetkovic, B. Xu, and P. Fontana, 2012, Analysis of a broadband processing technology applicable to conventional streamer data: 74th Annual International Conference and Exhibition incorporating SPE EUROPEC, EAGE, Extended Abstracts, I06.
Ziolkowski, A., 1970, A method for calculating the output pressure waveform from an air gun: Geophysical Journal of the Royal Astronomical Society, **21**, 137–161, doi: 10.1111/j.1365-246X.1970.tb01773.x.
Ziolkowski, A., G. E. Parkes, L. Hatton, and T. Haugland, 1982, The signature of an air gun array: Computation from near-field measurements including interactions: Geophysics, **47**, 1413–1421, doi: 10.1190/1.1441289.